

## Magnetic connections across the chromosphere-corona transition region

PHILIP JUDGE<sup>1</sup>

<sup>1</sup>*High Altitude Observatory, National Center for Atmospheric Research, Boulder CO 80307-3000, USA*

### ABSTRACT

The plasma contributing to emission from the Sun between the cool chromosphere ( $\leq 10^4$ K) and hot corona ( $\geq 10^6$ K) has been subjected to many different interpretations. Here we look at the magnetic structure of this transition region (TR) plasma, based upon the implications of CLASP2 data of an active region recently published by Ishikawa et al., and earlier IRIS and SDO data of quiet regions. Ishikawa et al. found that large areas of sunspot plages are magnetically unipolar as measured in the cores of Mg II resonance lines, formed in the lower transition region under low plasma- $\beta$  conditions. Here we show that IRIS images in the line cores have fibrils which well aligned with the overlying coronal loop segments seen in the 171 Å channel of SDO. When the TR emission in active regions arise from plasma magnetically and thermally connected to the corona, then the line cores can provide the first credible magnetic boundary conditions for force-free calculations extended to the corona. We also re-examine IRIS images of dynamic TR cool loops previously reported as a major contributor to transition region emission from the quiet Sun. Dynamic cool loops contribute only a small fraction of the total TR emission from the quiet Sun.

**Keywords:** Sun: atmosphere - Sun: chromosphere - Sun: transition region - Sun: corona - Sun: magnetic fields

### 1. INTRODUCTION

Ultraviolet emission from features formed between the  $\approx 6000$  K and  $10^6$  K plasmas of the chromosphere and corona of the Sun have been studied quantitatively for over half a century (e.g. Detwiler et al. 1961; Pottasch 1964; Burton et al. 1967). The underlying chromosphere spans many pressure scale heights, it is a thermostat in that an increase in heating there leads largely to the increased energy of latent heat of ionization of hydrogen, and the accompanying freed electrons lead to rapid radiation losses through inelastic collisions with atoms and atomic ions. In contrast, the overlying corona conducts heat more efficiently to lower temperature plasma than it can radiate, because abundant ions (particularly of H, He, C, N, O) are fully ionized, or belong to H- or He- like ions. Radiative losses from these ions are modest, because almost as much energy is required to excite radiative transitions, requiring a change in principal quantum number, as it does to ionize them (Gabriel & Jordan 1971, reviewed by Judge 2019). Therefore,

any coronal heating which would otherwise raise coronal temperatures is instead rapidly ducted to plasma at lower temperatures. The radiation losses per particle peak near the middle of the transition region close to  $10^5$  K, where transitions with no changes of principal quantum number, such as O VI and other members of, for example, Li-, Be-, B-, Na- like ions, efficiently emit UV radiation.

Increased heating in the corona therefore leads to larger TR radiative losses predominantly at UV wavelengths, with minor increases in coronal temperature (Woolley & Allen 1950). This physical scenario leads to well-known “scaling laws” for coronal loops close to equilibrium conditions, which are non-linear in electron temperature (McWhirter et al. 1975; Rosner et al. 1978).

The solar TR plasmas, when in thermal contact with both chromosphere and corona, are therefore sandwiched between two stable thermal reservoirs, but in itself tends to be unstable to modest perturbations. Consequently, little plasma can exist for long at intermediate temperatures near  $10^5$ K (Mariska 1992). For example in 1D empirical models, TR plasma spans of order 100 km in height, compared with 1500 km for the stratified chromosphere and many thousands of kilometers in the corona (e.g., see the review by Jordan 1992). Further,

it has been known for 7+ decades that static equilibria are impossible by consideration of radiative and classical conductive energy transport alone (Giovannelli 1949).

TR radiation generally emerges in the vacuum UV ( $\lambda > 1100 \text{ \AA}$ ) where normal incidence optics can be used, and in this region many space-based instruments have operated since the 1960s. As a consequence of the above considerations, the TR has been a natural focus of observers to focus on the dynamics and overall behavior of TR plasma as it spectacularly reacts to modest changes in conditions above and below. To the observer then, the TR appears very dynamic, akin to the motions at the end of a whip, in response to drivers above and below. The dynamic spectra of TR lines (e.g. Dere et al. 1989) have received an unusual amount of attention compared with their relatively benign chromospheric and coronal counterparts (Mariska 1992).

### 1.1. *The purpose of the present work*

In the light of new results of magnetic field measurements above the active corona reported by Ishikawa et al. (2021), we re-open an old debate concerning the magnetic and thermal structures that lead to TR emission. There are two camps of thought.

1. The TR plasma’s bright emission is caused by magnetic field-aligned transport processes, including but not limited to classical heat conduction down from the corona.
2. The TR plasma’s bright emission comes from an “unresolved fine structure” (henceforth “UFS”) in which the coronal energy flux does not contribute significantly to the emission, at least for plasmas below  $\approx 2 \times 10^4 \text{ K}$ . Instead the energy is supplied by upward directed mechanical energy, deposited locally and advected and radiated away.

The consequences of resolving this debate extend beyond studies of the TR. There is intense interest in understanding coronal physics as it pertains to the irradiation of interplanetary space with variable UV and X-ray radiation, as well as to the ejection of plasma and magnetic fields. Lines known to form in TR plasma formed under scenario 1. can be used to infer magnetic energy, configurations, and evolution in the overlying corona. TR emission arising from scenario 2. can say nothing about evolving magnetic properties of the corona.

### 1.2. *Field-aligned transport models*

In favor of models within camp 1., are two facts related to the differential emission measure. This well known quantity, derived by inversion of observations,

can be related to the energy balance, including its transport, across the TR. Jordan (1980). First the *shape* of this function derived from observations of quiet Sun, coronal holes and active regions is remarkably constant (e.g. Noyes et al. 1970; Jordan 1980; Feldman et al. 2009). This suggests a connection in the transport of energy across the chromosphere-corona transition (Jordan 1992). Secondly, above  $10^5 \text{ K}$ , the emission measure derived from observations varies as  $T_e^{5/2}$  with  $T_e$  the plasma electron temperature. This result is expected when energy is dominated by field-aligned heat conduction downwards (i.e. a constant conductive energy flux downwards, e.g. Jordan 1980). However, the emission measure structure below  $10^5 \text{ K}$  leads to TR emission that is far brighter than classical models, based on heat conduction, could predict (Kopp & Kuperus 1968). In principle this problem might be partly resolved in “funnel-like” expansion of the magnetic field Gabriel (1976). But in strong field concentrations where expansion has occurred below in the chromosphere, some have asked the question as to where the excess conducted energy goes (e.g. Kopp & Kuperus 1968; Athay 1990). The lack of static solutions identified first by Giovannelli (1949) has suggested to some that the excessively steep temperature gradients implied in classical models leads to dynamical instabilities (e.g., turbulence) which can then transport the conductive heat flux excess across the atmosphere in a quasi-steady manner. The elementary plasma physics of the consequences of the high conductive flux has been carefully discussed by Ashbourn & Woods (2001). A phenomenological formalism based on eddy diffusion was given by Cally (1990) in which the observed emission measures were used to find parameters of turbulent energy transport downwards to  $10^4 \text{ K}$ . An alternate picture involving steady flows has been invoked by Fontenla and colleagues who added neutral-ion diffusion processes (“ambipolar” diffusion) to develop sophisticated models in a plane-parallel configuration (Fontenla et al. 1990, 1993; Fontenla et al. 2002). Some have suggested that spicules might arise from effects of this heat flux (Kuperus & Athay 1967; Kopp & Kuperus 1968; Athay 2000).

Athay (1990) proposed that field-aligned transport of conductive energy, when it reaches cool plasma, may account for the emission measures below  $10^5 \text{ K}$ . Athay invokes a highly corrugated (non-horizontal) thermal interface, generated perhaps by the interface between the corona and embedded spicules. In this fashion, large cross-field temperature gradients may transport heat from hot coronal ions into those in the cooler plasma via ion-neutral collisions or anomalous cross-field transport processes (see also Ji et al. 1996; Judge 2008).

**Table 1.** IRIS 1400Å slitjaw image sequences

Start time UT	$N_{exp}$	X	Y	exp.	cadence	$\overline{DN/sec}$	$\bar{I}$	SSN
2013-10-02 06:47:23.5*	100	1	948	2.0	11.8	19.5	2093	107
2013-12-09 23:33:46.8*	128	970	30	8.0	18.9	75.8	2038	108
2013-09-13 06:36:51.6	300	-2	7	2.0	3.8	24	2560	105
2013-12-01 00:42:38.7	550	-3	3	2.0	3.8	15.3	1643	108
2017-04-03 07:40:01.0	640	-2	4	15.0	16.9	17.1	245	25
2019-07-05 09:39:36.5	590	2	-6	8.0	11.2	4.2	112	4
2019-07-08 09:49:21.4	600	2	-6	8.0	11.2	4.4	118	4
2019-07-11 17:19:23.4	128	1	-2	8.0	37.4	3.2	85	4

\*These are two of the datasets examined by [Hansteen et al. \(2014\)](#).  $N_{exp}$  is the number of slitjaw frames obtained, X and Y are coordinates of the center of the frames in arcsec, exposure time (exp.) and cadence are in seconds, the mean intensity  $\bar{I}$  is in  $\text{erg cm}^{-2} \text{s}^{-1} \text{sr}^{-1}$ . SSN is the monthly sunspot number compiled by Space Weather Services.

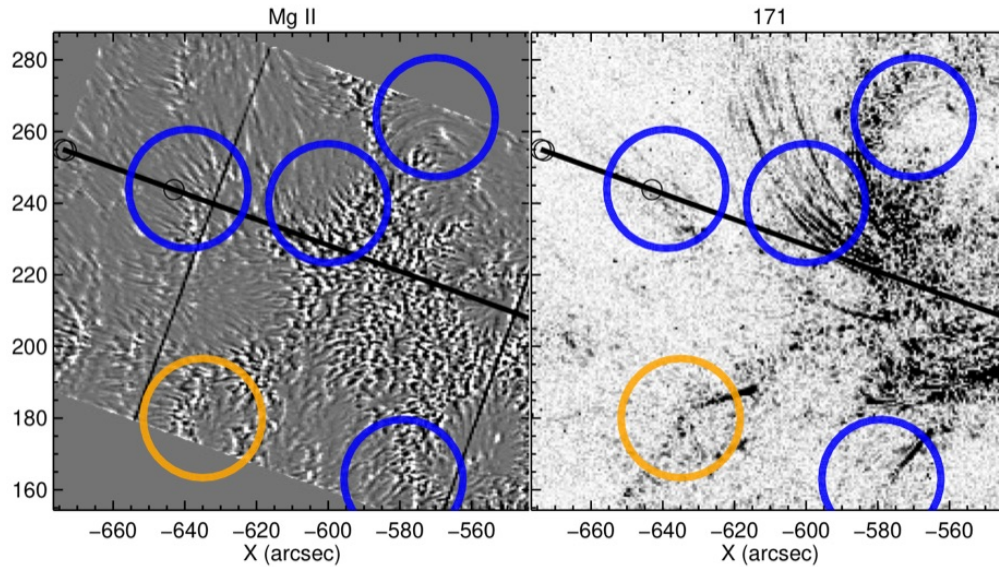


**Figure 1.** Edge-enhanced images from near the core of the Mg II k line (left panel, from an IRIS raster on 2019 April 11 from 15:57:54 to 16:25:26 UT) and in the AIA 171 Å channel (right panel, 16:53:33 UT) are shown. The images are from times close to the CLASP2 observations of [Ishikawa et al. \(2021\)](#). The central part of these images is all of the same magnetic polarity as measured using CLASP2 data by [Ishikawa et al. \(2021\)](#) in the Mg II lines. The black line shows the locus of the CLASP2 slit, the two small black circles correspond to the regions e and d of the chromospheric “network” identified by [Ishikawa et al. \(2021\)](#). Large blue circles show areas where the chromospheric fibrils and coronal loops appear well aligned, the orange circle shows a location where they are not.

### 1.3. Models for the TR “unresolved fine structures”

In an intriguing series of papers, Feldman has argued that the bright TR emission observed is from structures which are energetically disconnected from the corona (Feldman 1983, 1987, 1998). Given that the thermal conductivities along the magnetic field are many orders of magnitude greater than cross-field values at coronal temperatures, any bundles of magnetic flux which never reach coronal temperatures will remain thermally pro-

tected from coronal plasma in which they may be embedded. Qualitative physical interpretations by [Dowdy et al. \(1986\)](#) proposed that much of the quiet solar TR emission we see is not the result of downward energy transport. Instead the structures are a population of “cool loops”, with temperatures up to ca.  $10^5$  K, near the peak of the radiative loss function, in which local mechanical heating from below leads to the observed TR radiative losses. [Antiochos & Noci \(1986\)](#) were able to

relate the ideas to definite physical models based upon physical force and energy balance. They argued that cool loops could, under reasonable conditions, explain long-recognized problems associated only with classical heat transport along hot loops. Various authors studied the stability of such solutions (e.g. Cally & Robb 1991; Sasso et al. 2015), raising questions as to the viability of the model. However, this picture received support from the high resolution UV observations from the IRIS spacecraft, revealing dynamical closed loop-structures at the solar limb in spectral features formed in the lower TR of the quiet Sun (Hansteen et al. 2014, henceforth “H2014”). The thermal evolution of the loops observed by Hansteen et al. (2014) appears to vary on timescales of a minute or so, comparable to sound crossing times. Thus these emitting structures are not static and instability may not be an issue. In fact these structures are perhaps akin to the proposal of Sasso et al. (2015) in which populations of quasi-static models (those with subsonic speeds) might account for a variety of important observations.

In the UFS picture, the question remains as yet unanswered: how can the emission measure distributions both below and above  $10^5$  K be correlated, as observed, in this “cool loop” picture? Presumably some kind of statistical averaging is invoked. It is certainly true that the cool loops of H2014 are small, effectively below the resolutions of data used for most emission measure analyses, suggesting large numbers of small features will contribute over large areas. The question remains open.

Another question pertains to the nature of TR structures in *active regions*. In plages surrounding sunspots, the TR emission is on average several times brighter than in quiet regions (e.g. Brueckner & Bartoe 1974). Cool loops seen during the SKYLAB era in active regions (reviewed by Jordan 1976) might suggest that these structures again dominate the TR emission. These appeared most prominently under post-flare conditions. Later results from the VAULT  $L\alpha$  imager (Patsourakos et al. 2007) appeared to show cool loops associated with plages surrounding active regions. However, plages are known to be largely unipolar (Giovannelli 1982). Thus Judge & Centeno (2008) examined the underlying magnetic fields and the morphology of the  $L\alpha$  images, concluding instead that these cannot be cool loops because plages underlying VAULT images are indeed unipolar, as measured using sensitive magnetographs. The authors suggested instead that the TR over plages forms through energy transport from both the chromosphere and corona.

## 2. IMPLICATIONS OF DATA FROM THE CLASP2 UV SPECTROPOLARIMETER

The first published results from the CLASP2 mission (Ishikawa et al. 2021) focus on the Stokes  $V$  profiles of the resonance lines of Mg II as observed primarily in plages. Their results are important for our study of the TR, to include both active and quiet regions. While the bulk of the radiation in the opacity-broadened Mg II  $h$  and  $k$  lines is emitted from the chromosphere (Ayres 1979), the very cores form in plasma close to  $2 \times 10^4$  K in 1D models of Fontenla et al. (1993) (Judge et al. in preparation). These line cores can therefore probe magnetic conditions in the lower TR plasma. The calculations of line core formation heights in the 3D dynamical snapshots of Leenaarts et al. (2013) are unfortunately not plotted as a function of electron temperature  $T_e$ . But when the  $h$  and  $k$  lines become optically thin because of increased ionization to  $\text{Mg}^{2+}$  by electron collisions and not simply the drop in opacity when  $\text{Mg}^+$  is the dominant ion, then the  $\tau = 1$  surface must occur close to  $2 \times 10^4$  K. The contours of the  $\tau = 1$  surfaces of Mg II  $k$  in Figure 1 of Leenaarts et al. (2013) lie close to the  $2 \times 10^4$  K temperature cutoff shown, seeming to confirm this picture.

Judge & Centeno (2008) studied the morphology and the underlying photospheric magnetic environment of VAULT  $L\alpha$  data. They argued that the cool loop solutions cannot be important as active region TR contributors for several reasons. Firstly, the photospheric magnetic fields underlying the bright and curious  $L\alpha$  structures in the images appear unipolar. The unipolar fields measured using the Kitt Peak Vacuum Telescope (KPVT), had an average flux per resolution element of  $\approx 1.4 \times 10^{18}$  Mx. In contrast, the smallest detectable flux concentrations of opposite sign to the major polarity were  $1.3 \times 10^{16}$  Mx (a  $2\sigma$  statistical level). Although it is possible to hide the magnetic footpoints of loops if they are below this level, the Sun would have to arrange to do so such that *essentially no* flux of opposite polarity could be detected over an entire plage. One might expect, based upon the disorder associated with magneto-convection, that patches of opposite polarity, if present with sufficient flux, should be visible.

Judge & Centeno (2008) also argued that the morphology and spatial alignment of the  $L\alpha$  “fibrils” arranged themselves more like little comets, with tails somehow aligned over large areas. This situation is anything other than that envisaged for the quiet Sun (Dowdy et al. 1986).

The CLASP2 data sample magnetic fields directly at the base of the solar transition region. Such plasma is many orders of magnitude lower in pressure than, and



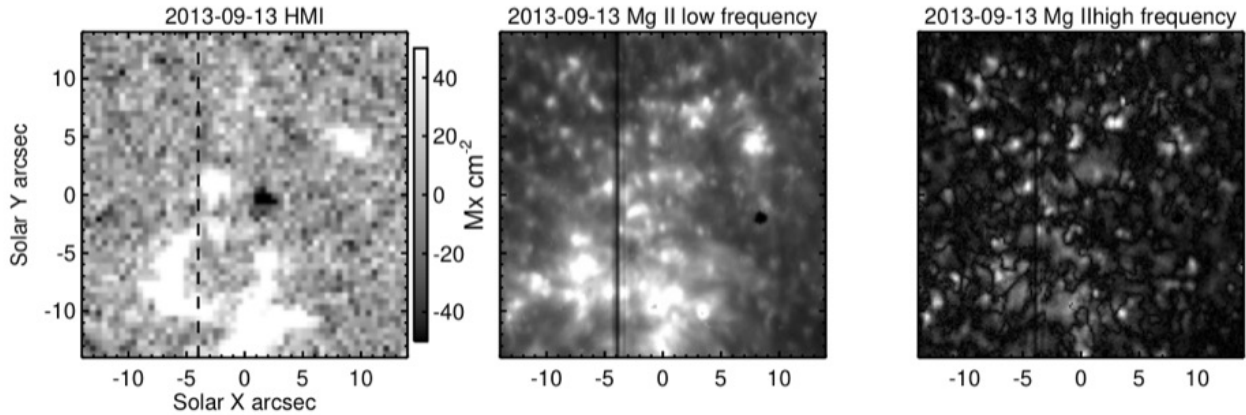


**Figure 2.** The left panel shows an HMI magnetogram obtained several minutes before the frequency-filtered 1400Å slitjaw images in the right panels were obtained at disk center on 2013-09-13 near to sunspot maximum. The middle panel shows the intensity in all features where the dominant power is at frequencies below 8 mHz (a period of 120 seconds). The right power shows the absolute value of power at high frequencies ( $> 8$  mHz). The morphology is slightly different in the HMI image because of the difference in timing of the order of tens of minutes between the HMI and IRIS timeseries of observations. The area shown is about the same as one supergranule. This is an area considered as “quiet” even though it was obtained when the Sun was relatively active.

$\approx 2$  Mm above, the photosphere where previous magnetic measurements have been made. The Stokes  $V$  profiles detected using CLASP2 in the observed plages and active network are *all of the same sign*. In any model of the Zeeman effect (Ishikawa et al. 2021 interpreted the data quantitatively using the weak field approximation), this can only mean unipolar line-of-sight (LOS) fields. The CLASP2 results are consistent with the physical picture of magnetic field decreasing in strength from their origins beneath the solar surface.

Following Judge & Centeno (2008), in Figure 1 we attempt to reveal possible alignments between the comet-like Mg II fibril structures at the edges of the plage and in the network to the west, with overlying coronal structure. A 1:1 correspondence between the two is not seen, but this is as expected given the disparate lengths and heights of the two kinds of structures. The Mg II “fibrils” are seen only at the edges of the plages. This is perhaps due to the dimmer background intensities over the quieter regions, and/or the denser populations and hence confusion expected over the central area of plages. Nevertheless, given the different projections of the chromospheric and coronal structures, the overall alignment is remarkable in the underlying organized directions along which magnetic structures can be traced.

We conclude that the evidence for the connection of bright plages and associated bright network emission in TR lines to the corona is definitive.

### 3. ANALYSIS OF IRIS DATA OF THE QUIET SUN TRANSITION REGION

Here we examine more IRIS data from the 1400 Å channel of the Slit Jaw Imager (SJI). We will conclude that indeed dynamic cool loops found by H2014 contribute to the quiet Sun’s emission in the resonance lines of Si IV, formed in the middle TR near  $10^{4.8}$  K. However, we will also find that the statistics of dynamical cool loops identified by H2014 indicate that these structures contribute far less than 50% to the emission from the quiet Sun. This stands in contrast to the claim by H2014:

IRIS observations prove that a large fraction of the solar transition region emission is due to low lying, relatively cool, loops having no thermal contact with the corona.

Firstly we examine the actual data analyzed by H2014, listed along with other data listed in Table 1. The data of H2014 were data taken at the solar limb, from October and December 2013, a period near the maximum of solar cycle 24. From histograms of properties of these dynamic loops (their Figure 2), we adopt the following numbers for analysis. The median values of apparent length, height above limb and intensity (in DN  $\text{sec}^{-1}$ ) are 4 Mm, 2 Mm and  $\approx 40$  DN  $\text{sec}^{-1}$  respectively. A distribution of lifetimes is not shown, but we assume that the time series shown in Figure S1 are typical, and estimate median lifetimes of order 60 seconds. This number is mentioned in their text as

...loops appear to be lit up in segments, with each segment only being visible for roughly a minute.

We will require two more statistical quantities- the number of cool loops visible at any time per unit arc length along the limb, and their apparent area in the plane of the sky. These quantities are not specified in the original paper but inspection of the limb and inside-limb images (their Fig. 1) indicates to us that there are at most 3 such loops visible over the quiet Sun limb every arc-minute of arc length (i.e., one such loop every length  $s \approx 14$  Mm). While this number is subject to large uncertainties given the published analysis, movie S1 of H2014 seems to confirm this rough number. Certainly in the data shown, the number cannot be twice this value for the regions shown. The loops shown in their Fig. 1 indicate a median loop area  $A$  of  $\approx 4 \cdot 0.5 = 2$  Mm<sup>2</sup>.

Let us transform the limb loops to disk center in a statistical sense. The geometry at the limb means that features of median height  $h$  will be visible if it lies within a line-of-sight length

$$\ell \approx \sqrt{2R_{\odot}h} \approx 50 \text{ Mm} \quad (1)$$

The equivalent area observed at disk center in the quiet Sun containing just 1 dynamic loop is then  $\ell \cdot s \approx 700$  Mm<sup>2</sup>. The area of a single supergranule is roughly 700 Mm<sup>2</sup>. We should expect to observe one of these bright loops per supergranule at any given time.

The total radiative flux from these features, assuming they are optically thin, is independent of viewing angle. Using the reported median intensity of UFS at the limb of  $I = 40$  DN sec<sup>-1</sup> (H2014), we would compute a mean disk-center intensity  $\bar{I}$  distributed over area  $\ell \cdot s$  of

$$\bar{I} \approx AI/(\ell \cdot s) \approx 0.003I \quad (2)$$

H2014 give a physical conversion of 215 erg cm<sup>-2</sup> sr<sup>-1</sup> s<sup>-1</sup> for each DN per second, so that  $I \approx 8600$  erg cm<sup>-2</sup> sr<sup>-1</sup> s<sup>-1</sup>. Taken together, we find that the summed intensity of all the limb cool loops when viewed at disk center in the 1400Å channel of the SJI is then

$$\bar{I} \approx 26 \text{ erg cm}^{-2} \text{ sr}^{-1} \text{ s}^{-1} \quad (3)$$

which includes both lines of Si IV. Perhaps some of the limb emission is hidden behind the extra opacity near 1400Å along such long lines of sight. In the Discussion section below, we relate the limb lines of sight to disk center and address attenuation by bound-free opacity of neutral silicon.

What might these structures then contribute to the quiet Sun intensities seen at disk center? To avoid inter-calibration issues, we examined disk center data from

IRIS acquired with the 1400Å SJI channel listed in Table 1. These sample various levels of sunspot activity from nearly maximum sunspot number of over 100 down to 4 per month. Clearly the mean disk center intensities vary greatly depending on the magnetic flux at disk center, for which the monthly SSN is a crude measure. Even though Sun center is often used to observe typical “quiet Sun” conditions, in the IRIS SJI images there is no typical value. Nevertheless, every case we have examined has significantly higher intensities than estimated from equations (1) – (3), even those at sunspot minimum which represent really quiet Sun.

Are these SJI intensities comparable to previous measurements of “average quiet Sun” intensities of TR lines at disk center? The “averages” are rather poorly defined because the rms spatial variations in Si IV lines are on the order of the mean values (Athay & Dere 1991). Nevertheless, the SUMER atlas of the quiet Sun has  $\bar{I} \approx 260$  erg cm<sup>-2</sup>sr<sup>-1</sup>s<sup>-1</sup> (Curd et al. 2001). Brekke’s atlas of HRTS data has  $\bar{I} \approx 170$  (Brekke 1993). All these estimates are at least an order of magnitude larger than the summed contributions of the limb dynamic loop intensities, using the above parameters.

To check this analysis, we filtered the disk center IRIS data in time using a filter centered at 120 seconds, twice the lifetime of the dynamics loops. The time series SJI frames analyzed here and by H2014 are between 3.8 and 18.9 seconds. Low-pass data were generated using a Gaussian filter to remove dynamic variations on time scales of 1 minute. The resulting low-pass time series was then subtracted from the initial data to produce a high-pass time series and the low- and high- bandpass datasets compared. Typical results for data obtained in 2013 are shown in figure 2. The data obtained near sunspot maximum, show features at low frequencies with intensities up to  $2 \times 10^4$  erg cm<sup>-2</sup>sr<sup>-1</sup> s<sup>-1</sup>. The high frequency component has features only as bright as 800 erg cm<sup>-2</sup>sr<sup>-1</sup>s<sup>-1</sup>. Figure 3 shows similar data obtained close to solar sunspot minimum (from Jul 8 2019 with a monthly sunspot number of 4). This figure, covering about 4 supergranular areas, has a good example of what to expect from a cool loop (discussed below), near (X,Y=-17,+20).

In both cases the features with significant power at periods below 120 seconds (right hand panels) account for about 25% of the total power (including zero frequency).

We conclude that using representative properties of the dynamic loops identified by H2014, *the dynamic cool loops of H2014 are a small contributor to the total emission of the quiet Sun TR.*

#### 4. DISCUSSION

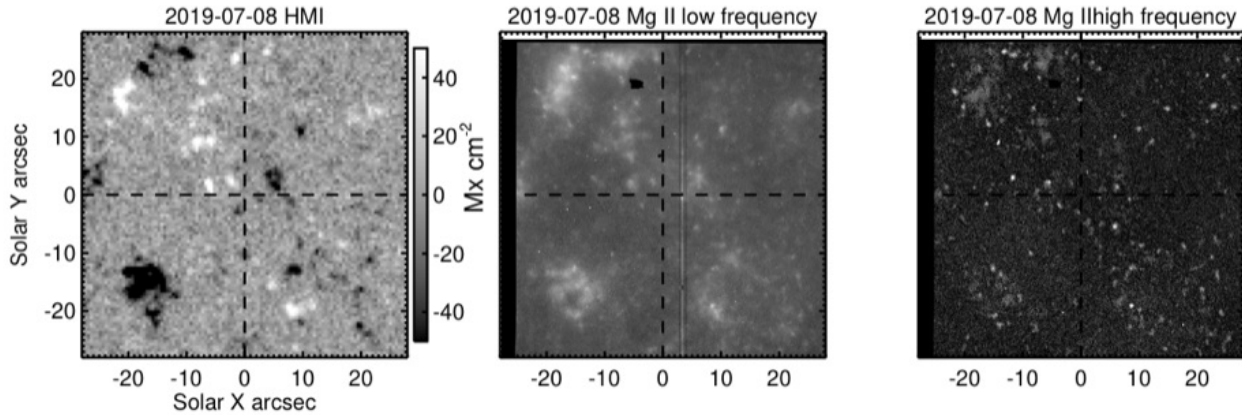


**Figure 3.** A figure identical to Figure 2 except that the data were acquired close to solar minimum conditions, it can be considered as “very quiet” Sun. “Cool loop” (dipolar) contributions are present near the top left of each panel, other areas of emission are more unipolar. Color scales are the same as for Figure 2. The lines help to reveal the precision of the alignment of the images.

#### 4.1. The active solar transition region

The conclusions of the analyses of Judge & Centeno (2008) and Ishikawa et al. (2021) appear unassailable. The active region plages consist of bright emission from with unipolar magnetic structures threading from chromosphere (or lower, perhaps) into the overlying corona, as inferred from Figure 1.

Readers may be surprised in that the TR associated with active regions is itself active (dynamic), with much evidence for magnetic reconnection (e.g. Dere et al. 1989). However, it should be remembered that reconnection will occur in unipolar magnetic fields which define the overall structure. Within these unipolar fields, tangential discontinuities (Parker 1988, 1994) are expected which can readily lead to reconnection not of the strong unipolar but the transverse components. This conclusion will modify some conclusions in the extensive literature (e.g. Mariska 1992, and later work).

The consequences of the work of Ishikawa et al. (2021) are particularly interesting for applications to understand the origin of flares, CMEs and other phenomena associated with the slow storage and sudden release of magnetic energy in the corona (Gold & Hoyle 1960). Measurements of magnetic fields in the lines of Mg II can be used to probe the magnetic structure and evolution as active regions evolve and release magnetic energy, plasma, radiation and perhaps magnetic helicity into interplanetary space.

#### 4.2. The “quiet” Sun

The main results of our study of quiet regions at disk center are based upon Figures 2 (a close-up of data

from Sep 13 2013 with a sunspot number of 105) and 4 (a larger view including TR and coronal AIA data from SDO). For comparison, and because the Sun center intensities measured by IRIS are a strong function of monthly sunspot number, Figure 3 shows similar data covering about 4 supergranule areas when the monthly sunspot number was 4. In all cases but one, the brightest 1400 Å emission lies directly above the HMI magnetograms of one polarity. The exception is the bipolar region of Figure 3 close to (X,Y=-17,+20) where emission at both high and low frequencies are seen spanning the opposite polarity regions. In the more active disk center data (Figure 4), the lower two panels reveal coronal structures: the He II channel formed near  $10^5$  K shows structure clearly associated with the Fe IX/X 171 Å coronal brightness. This again suggests an energetic connection of a unipolar region to the overlying corona. The spatial relationships are far from 1:1 because the coronal emission is spread along magnetic fields by efficient electron heat conduction.

But to what extent might there be direct evidence that the corona and the IRIS 1400 Å emission are energetically connected? The very different angular resolutions (0.32” for IRIS vs. 1” for SDO) preclude identifying the small bright IRIS structures with the overlying atmosphere. However, the white boxes in Figure 4 highlight some of the stronger regions of opposite polarity. Two such boxes (X=-6,Y=7 and X=11,Y=22) also include nearby positive polarity and so low-lying small loops might connect these regions. Indeed there is a small amount of Si IV 1400 Å emission present but this does not span from positive to negative polarity.

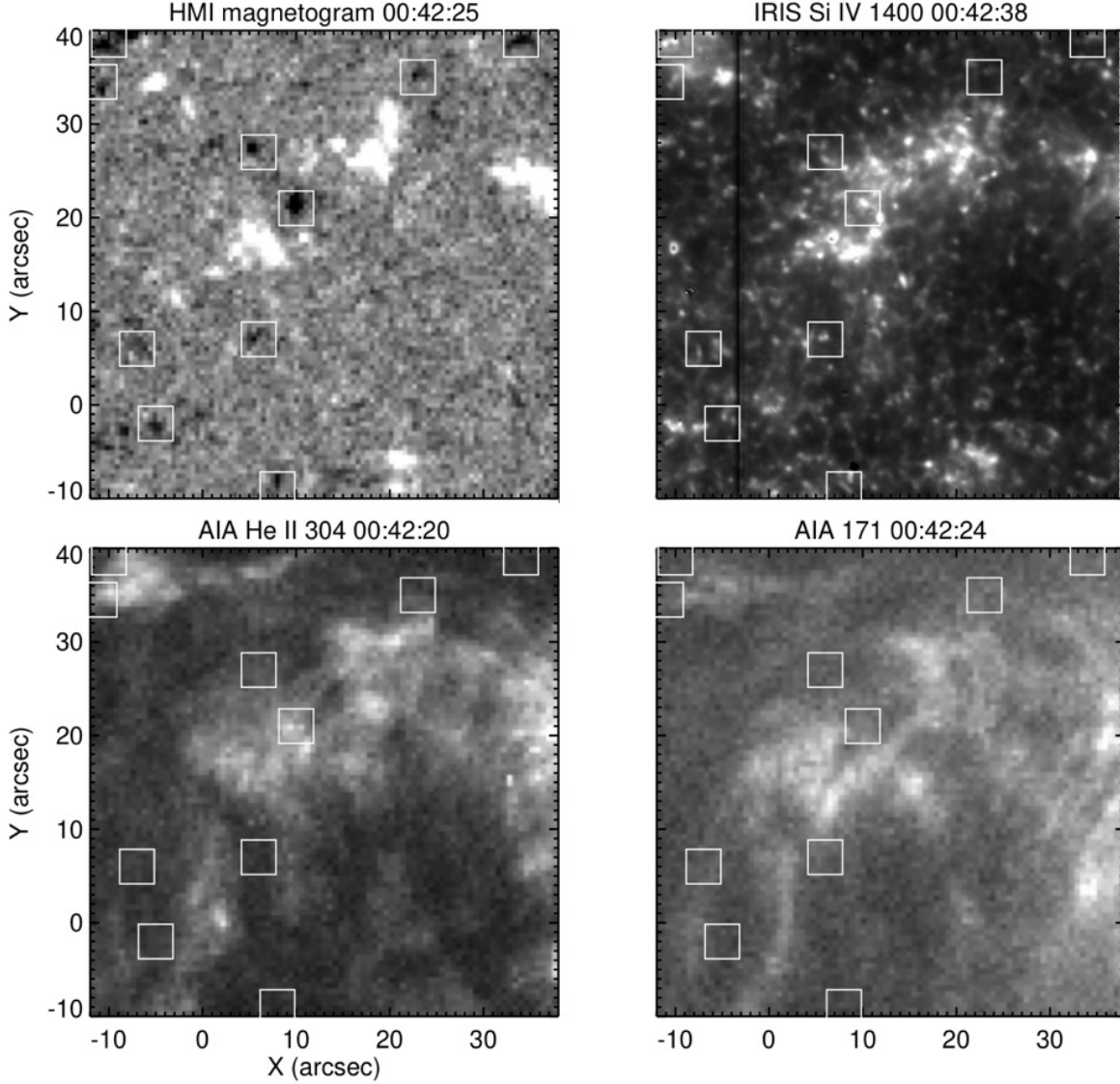


**Figure 4.** Various data obtained on December 1 2013 close in time to the first IRIS image of a sequence obtained at disk center. The area shown is roughly that of three supergranules. Synoptic views reveal this to be a quiet region, although with a monthly SSN of 108, the 1400 SJI data are quite bright compared with solar minimum conditions (Table 1). The images are co-aligned to within a second of arc. Some of the patches of negative polarity are marked with boxes for reference between images. The HMI magnetogram is saturated at  $\pm 40 \text{ Mx cm}^{-2}$ , the strongest flux concentrations range between  $-150$  and  $+100 \text{ Mx cm}^{-2}$ .

In these data there is therefore little indication of cool loop emission. This is as we expected on the basis of statistics of limb data obtained during the same season derived above (perhaps just one dynamic cool loop per supergranular area).

Our results for quiet regions appear to be self-consistent, with the possible exception of the N. polar sequence of frames acquired on 2013-10-02, with mean intensities equal to those of the scan on 2013-12-09 at lower latitudes. Perhaps these bright loops are related to

the roots of extended polar plumes which are magnetically multi-polar, relatively dense and themselves bright.

Here we find that the magnetic and IRIS data indicate that quiet Sun TR emission is dominated by plasma connected to the corona which, under typical coronal conditions, must lie near 2000 km above the photosphere. Spicular emission in TR lines will appear dominant at the limb because they are long and via equation (1) they are many times brighter than at disk center. This then raises the question, why then is the proposed bright TR



plasma connected to the corona not seen everywhere at the solar limb, for example in the data from Figure 1 of H2014?

We recall that absorbers at  $1400 \text{ \AA}$  are formed near heights of  $0.8 \text{ Mm}$  where  $\tau = 1$  vertically at disk center (opacity from neutral Si, Vernazza et al. 1981). At the limb, we can find a lower limit to the projected height at which the  $\tau = 1$  surface will arise assuming the atmosphere to be exponentially stratified. The density scale height  $h_c$  in the mid chromosphere of Vernazza et al. (1981) is about  $150 \text{ km}$ . Then, the limb path length tangential to the limb is  $\ell \approx \sqrt{2R_\odot h_c}$  is about  $15 \text{ Mm}$ , 100 times  $h_c$  (equation 1). The  $\tau = 1$  surface will be found at a projected high  $z$  above the disk center height of  $800 \text{ km}$ , when

$$\begin{aligned} \ell \cdot \exp(-z/h_c) &= 1, \text{ so that} \\ z &= 1400 \text{ km}, \end{aligned} \quad (4)$$

However, in these 1D models this height is limited not only by the height dependence of the density, but also by temperature since the coronal temperature rises to 1 million K near heights of  $2000 \text{ km}$  at disk center. Thus  $z$  is perhaps at most  $1200 \text{ km}$  in these models, and so any limb emission at heights  $\leq 800 + 1200 = 2000 \text{ km}$  will be attenuated. Given the presence of dynamic extensions higher than the hydrostatic scale heights (clearly shown in Figure 1 of Judge 2015 based upon data from the Bifrost code of Gudiksen et al. 2011), this is perhaps a lower limit. So, this is a minimal estimate of the attenuation of  $1400 \text{ \AA}$  radiation at the limb. Brighter TR emission lies below the  $2000 \text{ km}$  height (see the scaling laws for coronal pressure of McWhirter et al. 1975; Rosner et al. 1978 and the sequence of models A-F of Vernazza et al. 1981 for example). Not only this, but the presence of spicules and other cool material and the dynamic nature of the chromosphere in simulations means that the bulk of the bright TR emission at the footpoints of the corona will be mostly absent in the images analyzed by H2014.

There is qualitative agreement of the visibility of loops observed with IRIS and those in the numerical work of H2014. However, the initial mixed polarity state used

in these calculations maximizes the number of low-lying loops. Therefore these modeling efforts cannot be used to refute our conclusions.

Finally, CLASP2 data analyzed by Ishikawa et al. (2021) include regions of network (points d and e marked in their Figure 1 and Figure 3, and in this paper as small black circles in Figure 1). The Zeeman signals seen in the Mg II  $h$  and  $k$  line cores at these two locations are compatible with zero LOS magnetic field. The authors showed that these points are of opposite polarity in the photosphere with LOS average flux densities of  $\approx 220 \text{ Mx cm}^{-2}$ . Outside of the cores, the Mg II lines yielded  $160$  and  $80 \text{ Mx cm}^{-2}$  LOS flux densities in the lower and middle chromosphere respectively. Ishikawa et al. (2021) speculate that the non-detection may arise because associated loops may lie beneath the formation height of the line cores, because the magnetic flux densities lie below the Zeeman detection limit of  $\approx 10 \text{ Mx cm}^{-2}$ , or because the fields are perpendicular to the LOS. Here we can rule out the last possibility because local verticals at these points are inclined at  $\approx 43^\circ$  to the LOS, and any locally horizontal connecting loop structure between them would have to have as strong Zeeman component along the LOS as a vertical component. Until higher quality data and/or inversion scheme can be acquired, the precise meaning of these network observations for the conclusions of the present paper will remain unclear.

In conclusion, the bulk of transition region emission from quiet and active regions on the Sun does not arise from UFS, but from a magnetically-guided thermal interface between the corona and the chromosphere. This interface is probably highly corrugated, geometrically (see Figure 1, also e.g. Athay 1990; Ji et al. 1996; Judge 2008).

## ACKNOWLEDGMENTS

The author is grateful to Rebecca Centeno Elliott for reading the paper and for encouragement, and to an anonymous referee for very helpful comments. The National Center for Atmospheric Research is sponsored by the National Science Foundation.

## REFERENCES

- Antiochos, S. K., & Noci, G. 1986, *ApJ*, 301, 440, doi: [10.1086/163912](https://doi.org/10.1086/163912)
- Ashbourn, J. M. A., & Woods, L. C. 2001, *Proceedings of the Royal Society of London Series A*, 457, 1873, doi: [10.1098/rspa.2001.0791](https://doi.org/10.1098/rspa.2001.0791)
- Athay, R. G. 1990, *ApJ*, 362, 364
- Athay, R. G. 2000, *Sol. Phys.*, 197, 31
- Athay, R. G., & Dere, K. P. 1991, *ApJ*, 379, 776, doi: [10.1086/170553](https://doi.org/10.1086/170553)
- Ayres, T. R. 1979, *ApJ*, 228, 509
- Brekke, P. 1993, *ApJS*, 87, 443, doi: [10.1086/191810](https://doi.org/10.1086/191810)

- Brueckner, G. E., & Bartoe, J.-D. F. 1974, *Sol. Phys.*, 38, 133
- Burton, W. M., Ridgeley, A., & Wilson, R. 1967, *MNRAS*, 135, 207, doi: [10.1093/mnras/135.2.207](https://doi.org/10.1093/mnras/135.2.207)
- Cally, P. S. 1990, *ApJ*, 355, 693
- Cally, P. S., & Robb, T. D. 1991, *ApJ*, 372, 329
- Curdtt, W., Brekke, P., Feldman, U., et al. 2001, *A&A*, 375, 591
- Dere, K. P., Bartoe, J.-D. F., & Brueckner, G. E. 1989, *ApJ*, 345, L95
- Detwiler, C. R., Garrett, D. L., Purcell, J. P., & Tousey, R. 1961, *Annales de Geophysique*, 17, 263
- Dowdy, J. F., J., Rabin, D., & Moore, R. L. 1986, *Sol. Phys.*, 105, 35
- Feldman, U. 1983, *ApJ*, 275, 367
- . 1987, *ApJ*, 320, 426
- Feldman, U. 1998, *ApJ*, 507, 974
- Feldman, U., Dammasch, I. E., & Landi, E. 2009, *ApJ*, 693, 1474, doi: [10.1088/0004-637X/693/2/1474](https://doi.org/10.1088/0004-637X/693/2/1474)
- Fontenla, J. M., Avrett, E. H., & Loeser, R. 1990, *ApJ*, 355, 700
- . 1993, *ApJ*, 406, 319
- Fontenla, J. M., Avrett, E. H., & Loeser, R. 2002, *ApJ*, 572, 636
- Gabriel, A. 1976, *Phil Trans. Royal Soc. Lond.*, 281, 339
- Gabriel, A. H., & Jordan, C. 1971, *Case Studies in Atomic Collision Physics*, ed. E. McDaniel & M. C. McDowell (North-Holland), 210–291
- Giovanelli, R. G. 1949, *MNRAS*, 109, 372, doi: [10.1093/mnras/109.3.372](https://doi.org/10.1093/mnras/109.3.372)
- . 1982, *Sol. Phys.*, 77, 27, doi: [10.1007/BF00156093](https://doi.org/10.1007/BF00156093)
- Gold, T., & Hoyle, F. 1960, *MNRAS*, 120, 89
- Gudiksen, B. V., Carlsson, M., Hansteen, V. H., et al. 2011, *A&A*, 531, A154
- Hansteen, V., De Pontieu, B., Carlsson, M., et al. 2014, *Science*, 346, 1255757, doi: [10.1126/science.1255757](https://doi.org/10.1126/science.1255757)
- Ishikawa, R., Bueno, J. T., del Pino Alemán, T., et al. 2021, *Science Advances*, 7, doi: [10.1126/sciadv.abe8406](https://doi.org/10.1126/sciadv.abe8406)
- Ji, H. S., Song, M. T., & Hu, F. M. 1996, *ApJ*, 464, 1012, doi: [10.1086/177388](https://doi.org/10.1086/177388)
- Jordan, C. 1976, *Phil. Trans. R. Soc. London*, A281, 391
- . 1980, *A&A*, 86, 355
- Jordan, C. 1992, *Memorie della Societa Astronomica Italiana*, 63, 605
- Judge, P., & Centeno, R. 2008, *ApJ*, 687, 1388, doi: [10.1086/590104](https://doi.org/10.1086/590104)
- Judge, P. G. 2008, *ApJL*, 683, L87
- Judge, P. G. 2015, *ApJ*, 808, 116
- . 2019, Chapter 5 - Spectroscopy and Atomic Physics, ed. O. Engvold, J.-C. Vial, & A. Skumanich, 127–155, doi: [10.1016/B978-0-12-814334-6.00005-4](https://doi.org/10.1016/B978-0-12-814334-6.00005-4)
- Kopp, R. A., & Kuperus, M. 1968, *Sol. Phys.*, 4, 212
- Kuperus, M., & Athay, R. G. 1967, *Sol. Phys.*, 1, 361, doi: [10.1007/BF00151361](https://doi.org/10.1007/BF00151361)
- Leenaarts, J., Pereira, T. M. D., Carlsson, M., Uitenbroek, H., & De Pontieu, B. 2013, *ApJ*, 772, 90, doi: [10.1088/0004-637X/772/2/90](https://doi.org/10.1088/0004-637X/772/2/90)
- Mariska, J. T. 1992, *The Solar Transition Region* (Cambridge UK: Cambridge Univ. Press)
- McWhirter, R. W. P., Thoneman, P. C., & Wilson, R. 1975, *A&A*, 40, 63
- Noyes, R. W., Withbroe, G. L., & Kirshner, R. P. 1970, *Sol. Phys.*, 11, 388, doi: [10.1007/BF00153074](https://doi.org/10.1007/BF00153074)
- Parker, E. N. 1988, *ApJ*, 330, 474
- . 1994, *Spontaneous Current Sheets in Magnetic Fields with Application to Stellar X-Rays*, International Series on Astronomy and Astrophysics (Oxford: Oxford University Press)
- Patsourakos, S., Gouttebroze, P., & Vourlidas, A. 2007, *ApJ*, 664, 1214, doi: [10.1086/518645](https://doi.org/10.1086/518645)
- Pottasch, S. R. 1964, *Sp. Sci. Rev.*, 3, 816
- Rosner, R., Tucker, W. H., & Vaiana, G. S. 1978, *ApJ*, 220, 643
- Sasso, C., Andretta, V., & Spadaro, D. 2015, *A&A*, 583, A54, doi: [10.1051/0004-6361/201526598](https://doi.org/10.1051/0004-6361/201526598)
- Vernazza, J., Avrett, E., & Loeser, R. 1981, *ApJS*, 45, 635
- Woolley, R. V. D. R., & Allen, C. W. 1950, *MNRAS*, 110, 358, doi: [10.1093/mnras/110.4.358](https://doi.org/10.1093/mnras/110.4.358)